American Mineralogist, Volume 87, pages 1437–1442, 2002

Crystal chemistry of three tourmalines by SREF, EMPA, and SIMS

FERNANDO CÁMARA,[1] LUISA OTTOLINI,[1,*] AND FRANK C. HAWTHORNE[2]

[1]CNR-Instituto di Geoscienze e Georisorse (IGG), Sezione di Pavia, Via Ferrata 1, I-27100 Pavia, Italy
[2]Department of Geological Sciences, University of Manitoba, Winnipeg, MB R3T 2N2, Canada

ABSTRACT

The crystal structures of three tourmaline crystals: $(Na_{0.49}\ K_{0.01}\ Ca_{0.48})\ (Mg_{1.35}\ Fe^{2+}_{0.94}\ Fe^{3+}_{0.49}\ Ti_{0.20})\ (Al_{4.58}\ Fe^{3+}_{0.62}\ Mg_{0.80})\ (Si_{5.99}\ Al_{0.01})\ O_{18}\ (BO_3)_{3.03}\ (OH)_{3.18}\ F_{0.18}\ O_{0.64}$, a = 16.017(2), c = 7.256(2) Å, V = 1612.2(4) Å^3, $R3m$, Z = 3; $(Na_{0.64}\ K_{0.01}\ Ca_{0.03})\ (Mn_{0.18}\ Fe^{2+}_{1.71}\ Al_{0.88}\ Li_{0.11}\ Zn_{0.03}\ Ti_{0.07})\ (Al_{5.67}\ Fe^{3+}_{0.28}\ Mg_{0.05})\ (Si_{5.76}\ Al_{0.24})\ O_{18}\ (BO_3)_{2.99}\ (OH)_{3.96}\ F_{0.17}$, a = 15.983(2), c = 7.152(2) Å, V = 1582.1(4) Å^3; $(Na_{0.81}\ K_{0.01}\ Ca_{0.01})\ (Mn_{0.02}\ Mg_{0.61}\ Fe^{2+}_{0.90}\ Al_{0.80}\ Li_{0.70}\ Zn_{0.01}\ Ti_{0.06})\ Al_{6.00}\ (Si_{5.97}\ Al_{0.03})\ O_{18}\ (BO_3)_{2.93}\ (OH)_{3.42}\ F_{0.55}\ O_{0..03}$, a = 15.921(3), c = 7.137(2) Å, V = 1566.7(6) Å^3, have been refined to **R-**indices of 1.3–2.2% using X-ray intensity data collected with a four-circle diffractometer using Mo$K\alpha$ X-radiation. The crystals were analyzed by electron- and ion-microprobe techniques for all major and minor elements in the crystals. Unit formulae were calculated on the basis of 31 anions (O, OH, F) and the $Fe^{3+}/(Fe^{2+} + Fe^{3+})$ ratio was calculated for electroneutrality. The refined site-scattering values and the observed <Y-O> and <Z-O> distances were used to assign site populations that are in accord with the unit formulae calculated from the electron- and ion-microprobe compositions. The B contents are equal to 3.0 apfu (atoms per formula unit) within experimental error. In two of the crystals, (OH + F) = 4.0 apfu. However, the third crystal has (OH + F) = 3.36 apfu and O^{2-} is dominant at the W(O1) site, and is an "oxy" tourmaline as defined by Hawthorne and Henry (1999). Non-spherical electron-density was observed at the X site, suggesting that there is some positional disorder at this site associated with occupancy of X by Ca and Na, possibly coupled with variable anion occupancy of the O1 site.

INTRODUCTION

There has been much recent work on the crystal chemistry of tourmaline (Hawthorne 1996; Hawthorne and Henry 1999 and references therein) due to the application of new and more accurate analytical techniques (Foit and Rossenberg 1977; Povondra and Novák 1986; Hawthorne 1995; Hervig 1996; McGee and Anovitz 1996; Dyar et al. 1998; Ottolini and Hawthorne 1999; Ottolini et al. 2002) and the renewed interest in understanding phase relations of B-bearing minerals in igneous, sedimentary, and metamorphic rocks (Henry and Guidotti 1985; Povondra and Novák 1986; London et al. 1996; Grew 1996; Henry and Dutrow 1996; Henry et al. 1999). Hawthorne and Henry (1999) reviewed the crystal-chemical aspects of chemical substitutions and structural features in tourmaline. Several substitutions in tourmaline involve light elements, and heterovalent substitutions at anion sites cannot be identified easily without accurate analysis of H and F. Therefore, studies addressing higher accuracy in the determination of these elements in tourmaline are crucial to further the understanding of chemical substitutions and order-disorder schemes.

METHODS

Sample description and preparation

The three samples of tourmaline are from the Harvard Mineralogical Museum, and were kindly provided by Carl A. Francis and M. Darby Dyar. Crystal 1 is a fragment from a large crystal from Madagascar (Frondel et al. 1966). Crystal 2 is from a black nodule from the Alto Lighona pegmatite field, Zambezia, Mozambique. Crystal 3 is from a pegmatite at Minas Gerais, Brazil. Table 1 reports the sample names and crystal-structure refinement information. These same samples were analyzed by Dyar et al. (1998) (1,2,3 in their sample list), who examined a larger group of tourmaline samples by Mössbauer spectrometry, EMPA, SIMS, and H-line extraction. A complementary SREF study of some samples of this set (Bloodaxe et al. 1999) did not include the samples reported here.

The crystals selected for study were glued onto glass fibres, mounted on a Philips PW1100 4-circle diffractometer, and a complete data collection was done for each crystal.

The mounting procedure for chemical analysis is described in Ottolini et al. (2002).

Electron microprobe analysis (EMPA)

Electron microprobe analysis was done at the University of Manitoba and at the Geological Survey of Canada (Ottawa) on fully automated CAMECA SX50 instruments operating in wavelength-dispersive mode. For elements with $Z > 9$, the following conditions were used: excitation voltage = 15 kV; specimen current = 20 nA; peak-count time = 20 s; and background-count time = 10 s. The following standards for $K\alpha$ X-ray lines were used: P = VP_2O_7; Si = almandine; Al = kyanite; Ti = titanite; Fe = fayalite; Mn = spessartine; Zn = gahnite; Mg = forsterite; Ca = diopside; Sr = celestite; Na = albite; K =

* E-mail: ottolini@crystal.unipv.it

TABLE 1. Data collection and refinement information for tourmaline crystals of this study

Sequence*	gfj	gde	gen
Crystal no.	drv-18†	sch-16†	elb-19†
Sample	HS-108796 N.1	HS-112566 N.1	HS-98144 N.1
a (Å)	16.017(2)	15.983(2)	15.921(3)
c (Å)	7.256(2)	7.152(2)	7.137(2)
V (Å^3)	1612.2(4)	1582.1(4)	1566.7(6)
Space group	*R*3*m*	*R*3*m*	*R*3*m*
Z	3	3	3
Rad/Mon	Mo/Gr	Mo/Gr	Mo/Gr
θ range (°)	2.5-42	2.5-35	2.5-42
No. unique refl.	1430	903	1383
R_{sym}	1.6	2.1	4.4
R_{all}	1.3	1.4	2.2
wR_{all}	3.5	3.55	5.04
GOF*	1.137	1.108	1.104

* Sequence order in IGG database.
† Samples corresponds to the sample set described by Ottolini et al. (2002).
*GOF = goodness of fit.

TABLE 2. Chemical analyses (wt%) and mineral formulae (apfu) of the crystal studied

Crystal no.	1	2	3
SiO_2	34.86	34.07	36.75
B_2O_3	10.30	9.80	10.80
B_2O_3*	(10.21)	(10.25)	(10.45)
Al_2O_3	22.54	33.90	35.74
TiO_2	1.57	0.55	0.51
FeO_{tot}	14.51	14.10	6.62
FeO	6.67	14.10	6.62
Fe_2O_3†	8.70		
MgO	8.39	0.19	2.51
MnO	0.00	1.26	0.16
ZnO	0.00	0.28	0.05
Li_2O	(0.0016)	(0.168)	(1.07)
K_2O	0.06	0.05	0.03
CaO	2.58	0.14	0.08
SrO	0.00	0.00	0.00
Na_2O	1.48	1.95	2.56
F	0.33	0.32	1.08
F*	(0.295)	(0.304)	(1.07)
H_2O*	(2.77)	(3.51)	(3.16)
Total	100.16	100.74	100.77
O=F	0.14	0.13	0.45
Total	100.02	100.60	100.32
Si	5.99	5.76	5.97
Al		0.24	0.03
ΣT	5.99	6.00	6.00
B	3.03	2.99	2.93
Al	4.58	5.67	6.00
Fe^{3+}	0.62	0.28	
Mg	0.80	0.05	
Σ Z	6.00	6.00	6.00
Mg	1.35		0.61
Al	0.00	0.88	0.80
Ti	0.20	0.07	0.06
Fe^{2+}	0.94	1.71	0.90
Fe^{3+}	0.49		
Mn^{3+}	0.00	0.00	0.00
Mn^{2+}	0.00	0.18	0.02
Zn^{2+}	0.00	0.03	0.01
Li	0.00	0.11	0.70
Σ Y	2.98	2.99	3.10
Ca	0.48	0.03	0.01
K	0.01	0.01	0.01
Na	0.49	0.64	0.81
Σ X	0.98	0.68	0.83
F	0.18	0.17	0.55
OH	3.18	3.96	3.42
Σ W+V	3.36	4.13	3.98

* Values between parentheses represent SIMS data; mineral formulae calculated with SIMS data.
† Fe_2O_3 calculated with Fe^{3+}/Fe_{total} taken from Dyar et al. (1998) Mössbauer data for no. 1.
V, Cr not detected.

orthoclase; F = fluororiebeckite. Each grain was analyzed at a minimum of 25 points to check for compositional zoning and to obtain good counting statistics. Data were reduced using the method of Pouchou and Pichoir (1984, 1985).

For the analysis of B, the following conditions were used: excitation voltage = 10 kV; specimen current = 100 nA using a ~5 μm diameter beam spot; peak-count time = 200 s; and background-count time = 100 s. Dravite was used as standard for $^{[III]}$B. Data were reduced using the routine of Armstrong (1988). Chemical compositions and unit formulae are reported in Table 2.

Secondary-ion mass spectrometry (SIMS)

SIMS measurements were done with a Cameca IMS 4f microprobe at CNR-IGG (Pavia). We used a $^{16}O^-$ primary-ion beam with a current intensity of 1–1.5 nA, and a beam diameter less than 5 μm. There were three analytical sessions. The final results for Li and B are the average of all the data (typically four or five analytical points for each crystal) collected on the different runs over a period of one year; data for H and F were collected in two analytical sessions. A detailed description of the analytical conditions and quantification procedure is reported by Ottolini et al. (2002). Results for SIMS quantification using Si as the internal reference for the matrix are reported in parentheses in Table 2, together with the EMPA results. Mineral formulae were calculated on the basis of 31 (O, OH, F).

Single-crystal structure refinement (SREF)

Data collection and refinement were done for one crystal of each sample [crystals 1, 2, and 3, corresponding to samples drv-18, sch-16, and elb-19, respectively, in the sample-set described by Ottolini et al. (2002)] with an automated Philips PW1100 4-circle diffractometer using graphite-monochromatized Mo$K\alpha$ X-radiation. Unit-cell parameters were calculated from least-squares refinement of *d*-spacings calculated for 60 rows of the reciprocal lattice by measuring the reflections in the range $-35 < \theta < 35°$. They are reported in Table 1, together with other data-collection parameters. Reflection profiles were integrated following the method of Lehmann and Larsen (1974) as modified by Blessing et al. (1974). Intensities were corrected for Lorentz-polarization and absorption following North et al. (1968). Weighted full-matrix least-squared refinements were done using SHELX97 (Sheldrick 1997). Scattering factors were taken from the *International Tables for Crystallography* (Wilson 1995): neutral vs. ionized scattering-factors were used for O sites (Ungaretti et al. 1983), F vs. O^- at the V and W sites, and fully ionized scattering factors for all cations, except B. For B, a neutral scattering factor was refined against vacancy at the B site, to account for ionization effects.

Refined atom coordinates, isotropic and anisotropic-displacement parameters are shown in Table 3. Selected bond lengths are reported in Table 4. Table 5 reports the agreement between the refined-site scattering values at the X, Y, Z, V, and W

TABLE 3. Atom coordinates ($\times 10^4$) and equivalent isotropic and anisotropic-displacement parameters ($Å^2 \times 10^3$) for the crystals studied

	Crystal no.	*x*	*y*	*z*	U_{eq}	U_{11}	U_{22}	U_{33}	U_{23}	U_{13}	U_{12}
	1	1898(1)	1915(1)	732(1)	6(1)	5(1)	5(1)	6(1)	0(1)	1(1)	2(1)
T	*2*	1900(1)	1919(1)	393(1)	5(1)	5(1)	5(1)	6(1)	0(1)	0(1)	3(1)
	3	1899(1)	1919(1)	529(1)	4(1)	4(1)	4(1)	4(1)	0(1)	0(1)	2(1)
		8898(1)	1102(1)	6201(2)	7(1)	6(1)	6(1)	9(1)	–1(1)	1(1)	3(1)
B		8898(1)	1102(1)	5853(2)	7(1)	7(1)	7(1)	8(1)	0(1)	0(1)	3(1)
		8902(1)	1098(1)	5977(2)	6(1)	6(1)	6(1)	7(1)	0(1)	0(1)	3(1)
		0	0	8489(1)	18(1)	17(1)	17(1)	19(1)	0	0	8(1)
X		0	0	8186(4)	24(1)	24(1)	24(1)	24(1)	0	0	12(1)
		0	0	8189(3)	22(1)	25(1)	25(1)	16(1)	0	0	12(1)
		616(1)	9384(1)	4367(1)	9(1)	7(1)	7(1)	11(1)	–2(1)	2(1)	2(1)
Y		617(1)	9383(1)	4102(1)	9(1)	7(1)	7(1)	12(1)	–2(1)	2(1)	2(1)
		622(1)	9378(1)	4242(1)	7(1)	6(1)	6(1)	8(1)	–1(1)	1(1)	2(1)
		2619(1)	2983(1)	4611(1)	6(1)	6(1)	6(1)	6(1)	0(1)	–1(1)	3(1)
Z		2615(1)	2983(1)	4291(1)	6(1)	6(1)	6(1)	6(1)	0(1)	–1(1)	3(1)
		2611(1)	2978(1)	4414(1)	5(1)	6(1)	6(1)	4(1)	0(1)	–1(1)	3(1)
		0	0	2946(3)	16(1)	17(1)	17(1)	15(1)	0	0	9(1)
O1		0	0	2563(5)	37(1)	48(2)	48(2)	14(1)	0	0	24(1)
		0	0	2714(5)	45(1)	62(2)	62(2)	10(1)	0	0	31(1)
		9393(1)	607(1)	5955(1)	11(1)	11(1)	11(1)	13(1)	–1(1)	1(1)	8(1)
O2		9384(1)	616(1)	5560(2)	15(1)	21(1)	21(1)	12(1)	0(1)	0(1)	18(1)
		9389(1)	611(1)	5687(2)	14(1)	22(1)	22(1)	10(1)	0(1)	0(1)	20(1)
		1331(1)	8669(1)	5611(1)	13(1)	14(1)	14(1)	7(1)	1(1)	–1(1)	5(1)
O3		1344(1)	8657(1)	5300(2)	12(1)	12(1)	12(1)	7(1)	0(1)	0(1)	2(1)
		1343(1)	8657(1)	5432(2)	10(1)	10(1)	10(1)	6(1)	0(1)	0(1)	1(1)
		9078(1)	922(1)	19(1)	11(1)	8(1)	8(1)	11(1)	1(1)	–1(1)	0(1)
O4		9066(1)	934(1)	9704(2)	10(1)	8(1)	8(1)	9(1)	1(1)	–1(1)	1(1)
		9068(1)	932(1)	9822(2)	8(1)	7(1)	7(1)	7(1)	0(1)	0(1)	0(1)
		909(1)	9091(1)	9830(1)	10(1)	8(1)	8(1)	10(1)	1(1)	–1(1)	0(1)
O5		935(1)	9065(1)	9482(2)	10(1)	8(1)	8(1)	9(1)	0(1)	0(1)	0(1)
		932(1)	9068(1)	9603(2)	8(1)	7(1)	7(1)	7(1)	0(1)	0(1)	0(1)
		1866(1)	1954(1)	2935(1)	9(1)	9(1)	11(1)	7(1)	0(1)	1(1)	5(1)
O6		1877(1)	1978(1)	2642(1)	8(1)	10(1)	9(1)	6(1)	0(1)	0(1)	4(1)
		1870(1)	1971(1)	2768(1)	7(1)	9(1)	7(1)	4(1)	0(1)	0(1)	3(1)
		2837(1)	2842(1)	9933(1)	9(1)	7(1)	8(1)	11(1)	2(1)	1(1)	1(1)
O7		2859(1)	2854(1)	9602(1)	8(1)	6(1)	7(1)	8(1)	1(1)	1(1)	2(1)
		2857(1)	2855(1)	9727(1)	6(1)	6(1)	5(1)	6(1)	0(1)	1(1)	1(1)
		2698(1)	2090(1)	6313(1)	11(1)	10(1)	6(1)	17(1)	–1(1)	–3(1)	4(1)
O8		2708(1)	2099(1)	5990(1)	9(1)	10(1)	6(1)	11(1)	–1(1)	–2(1)	4(1)
		2706(1)	2099(1)	6115(1)	7(1)	10(1)	5(1)	8(1)	–1(1)	–3(1)	4(1)
		1329(12)	8671(12)	6780(50)	17(7)						
H3		1319(15)	8681(15)	6610(70)	23(10)						

Note: U_{eq} is defined as one third of the trace of the orthogonalized U_{ij} tensor. The anisotropic displacement factor exponent takes the form: $-2\pi^2[h^2a^{*2}U_{11} + \cdots + 2hka^*b^*U_{12}]$.

sites and the corresponding values calculated from the chemical formulae. Table 6[1] lists observed and calculated structure factors.

RESULTS AND DISCUSSION

The chemical compositions of the three crystals were characterized by three different methods, and the agreement among the data is excellent (Tables 2 and 5). Analysis for B by EMP can be affected by inaccuracies derived from standard calibration and crystallographic orientation of the sample. Furthermore, the presence of Cl may represent a problem for accurate background determination, as the Cl L_l and L_n lines are very close to the B$K\alpha$ lines in the X-ray spectrum, even when using LSM detectors (McGee et al. 1991). This interference may lead to wrong background estimation, producing spurious B_2O_3 values. Fortunately, Cl is not a significant component of tourmaline.

Combining the chemical information obtained by SIMS on light and volatile elements with SREF results, we can estimate the oxidation state of Fe. Our data disagree with the Mössbauer

[1]For a copy of Table 6, document item AM-01-016, contact the Business Office of the Mineralogical Society of America (see inside front cover of recent issue) for price information. Deposit items may also be available on the American Mineralogist web site at http://www.minsocam.org.

TABLE 4. Selected interatomic distances (Å) for the crystals studied

Crystal no.	1	2	3
T-O6	1.6020(7)	1.6122(10)	1.6013(10)
T-O7	1.6030(6)	1.6158(9)	1.6125(8)
T-O4	1.6327(4)	1.6264(5)	1.6246(5)
T-O5	1.6483(5)	1.6396(6)	1.6378(6)
<T-O>	1.6215	1.6235	1.6191
B-O2	1.3837(15)	1.362(2)	1.359(2)
B-O8 ×2	1.3729(9)	1.3835(13)	1.3845(11)
<B-O>	1.3765	1.3763	1.3760
X-O2 ×3	2.4937(12)	2.537(2)	2.455(2)
X-O4 ×3	2.7878(11)	2.8036(17)	2.8211(16)
X-O5 ×3	2.7038(10)	2.7494(17)	2.7605(16)
<X-O>	2.6618	2.6967	2.6789
Y-O3	2.1780(11)	2.1870(15)	2.1632(15)
Y-O1	1.9970(10)	2.0308(18)	2.0315(19)
Y-O2 ×2	2.0518(7)	2.0001(10)	1.9877(10)
Y-O6 ×2	2.0264(7)	2.0414(10)	2.0241(9)
<Y-O>	2.0552	2.0501	2.0364
Z-O6	1.9137(7)	1.8626(10)	1.8584(9)
Z-O8	1.9421(7)	1.9248(10)	1.9152(9)
Z-O3	1.9959(5)	1.9781(7)	1.9693(7)
Z-O7	1.9805(7)	1.9599(9)	1.9560(9)
Z-O7	1.9194(7)	1.8798(9)	1.8835(9)
Z-O8	1.9109(7)	1.8849(9)	1.8840(9)
<Z-O>	1.9438	1.9150	1.9111
O3-H3	0.85(4)	0.94(5)	

results published by Dyar et al. (1998) for crystal no. 3 (FeO = 2.37 wt%; Fe_2O_3 = 4.30 wt%). Applying their Fe^{3+}/Fe_{total} ratio, we obtain low contents of Li and H_2O, in clear disagreement with our SIMS values. For crystal no. 1, the reported ratio agrees better with our data, but it is probably lower than the true value, as we will discuss later.

Some of the crystals analyzed by Mössbauer in Dyar et al. (1998) were re-analyzed by SmX (synchrotron micro-X ray absorption near edge spectrometry) by Bloodaxe et al. (1999), giving significantly different Fe^{3+}/Fe^{2+} ratios. This difference could be due to sample inhomogeneity.

Our SIMS data agree with the B determination by SIMS of Dyar et al. (1998) within 3% relative for samples 2 and 3, and ~5% relative for sample 1. Our H_2O contents (derived by SIMS) are higher than those reported by Dyar et al. (1998) for those samples; the agreement is ≤11% relative for samples 1 and 3, and ~23% relative, for sample 2. Their H_2O estimation is probably too low, as it indicates (OH + F) < 4 apfu for crystals no. 2 and no. 3, which was not indicated in the present SIMS or SREF work. For crystal 2, our SIMS value for H_2O (3.51 wt%) is probably slightly too high. The difference between the observed and stoichiometric contents (3.39 wt% H_2O) is ~3% relative, within the uncertainty of our SIMS procedure in tourmaline (for details, see Ottolini et al. 2002).

Following the classification scheme of Hawthorne and Henry (1999), the high Fe content at the Y site and the high site-scattering at the X site (15.7 e–) due to 0.48 apfu Ca, indicates that crystal 1 is intermediate between feruvite and schorl. Crystal 2 is schorl, and crystal 3 is fluor-elbaite.

V and W sites

As indicated by Hawthorne and Henry (1999), the V site (O3) can be occupied by OH and O^{2-}, and the W site (O1) can be occupied by OH, F, and O^{2-} with the site preference V << W. In accord with this behavior, the OH contents of the three tourmaline crystals examined here have OH > 3 apfu, indicating that W = $(OH)_3$. Crystals 2 and 3 have (OH + F) ≈ 4 apfu, indicating that monovalent anions are dominant at O1, and crystal 1 is an "oxy" tourmaline (Hawthorne and Henry 1999).

No evidence of a clear residual maximum was found near the W site in two of the crystals investigated. Only a very weak maximum near the W site was detected for crystal 1. Significant occupancy of F is indicated at the W site for all three crystals from the refined-site scattering values (Table 5).

After refining the anisotropic-displacement parameters, a maximum at a distance of ~ 0.9 Å from the V site was found in the difference-Fourier maps of crystals 1 and 2. This maximum was assigned to the H3 site (Grice and Robinson 1989; Grice and Ercit 1993; Grice et al. 1993). In crystal 3, no maximum near to the V site was detected. The absence of this maximum may be due to the quality of the diffraction data for this crystal, which is the lowest of the three crystals studied (R_{sym} = 4.4).

Inspection of Table 3 shows a high U_{eq} for O1 in crystals 2 and 3. This feature is frequent in refined tourmaline structures, as discussed by Burns et al. (1994). Figure 1a shows an isotropic distribution of density in both (001) and (100) sections of crystal 1, corresponding to its low U_{eq} (0.016). Figure 1b and c show a 3-lobed character for (001) sections in crystals 2 and 3, similar to that reported by Burns et al. (1994) for manganiferous elbaite, with the lobes oriented in the directions of the adjacent Y sites. This positional disorder was interpreted by Burns et al. (1994) as the consequence of local ordered arrangements of Li, Mn^{2+}, and Al due to the Y site composition; for crystal 3, the Y site composition is $(Li_{0.70}Mg_{0.61}Fe^{2+}_{0.90}Al_{0.80})$, indicating similar disorder and perhaps explaining the high R_{sym} values for this crystal.

Difference-Fourier maps for the crystals also show similar electron density around the O1 site in crystals 2 and 3 (ca., 8 e–/A^3), indicating F or OH occupancy, in close agreement with the hydrogen determinations by SIMS. The electron den-

TABLE 5. Agreement between scattering of assigned site-populations (epfu) and refined-site scattering values (epfu)

	X site		Y site		Z site		V site		W site	
Crystal no.	X-ray	assigned	X-ray	assigned	X-ray	assigned	X-ray	assigned	X-ray	assigned
1	15.7(1)	15.2	19.6(1)	19.3	14.2(1)	14.2	8.0(1)	8.0	8.32(1)	8.2
2	7.9(1)	7.7	21.7(2)	21.1	13.6(1)	13.6	8.0(1)	8.0	8.65(2)	8.2
3	9.6(1)	9.3	14.9(2)	15.1	13.04(5)	13.0	8.0(1)	8.0	8.92(2)	8.6

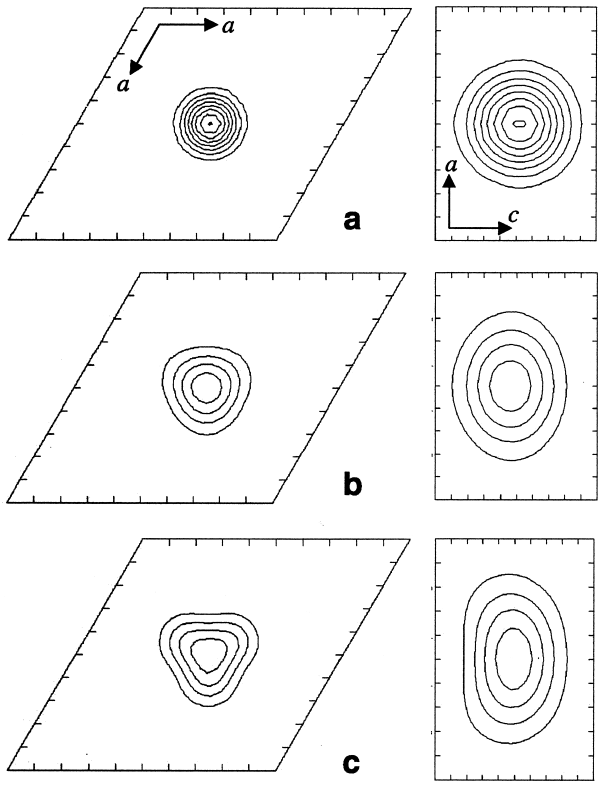

FIGURE 1. Difference-Fourier maps around the O1 site in the three crystals studied: (**a**) 1, (**b**) 2, and (**c**) 3. On the left are (001) sections; on the right are (100) sections. Contour interval = 2 e/Å^3; note the three-lobed pattern of electron density for crystals 2 and 3 in (001) section, and the elongation in two directions in the (100) sections for the same crystals.

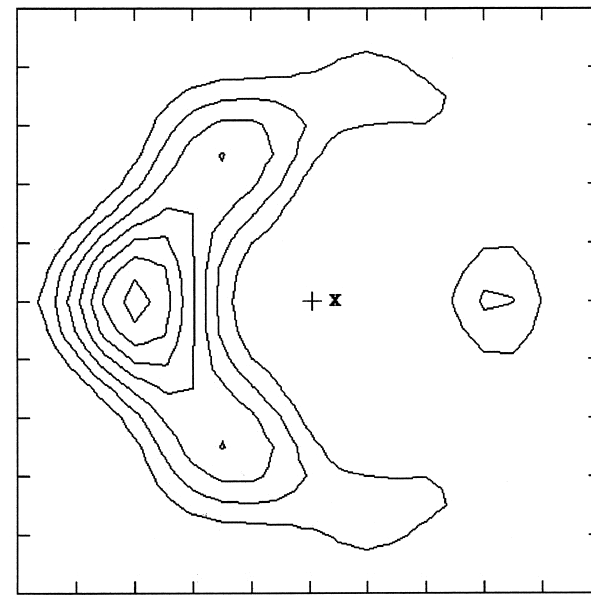

FIGURE 2. Difference-Fourier map for crystal 1, showing the splitting of the *X*-site along the *c* axis. Projection down the *X* axis. Contour interval = 0.1 e/Å^3.

sity at O1 is higher for crystal 1, in agreement with the presence of O^{2-} as indicated by SIMS H-analysis.

T and B sites

Refined site-scattering values at the B site show $^{[III]}$B to be stoichiometric in all three specimens. <T-O> bond-lengths indicate some Al substitution for Si in crystal 2. From Figure 2 of Hawthorne (1996), the T site is occupied by 5.8 Si apfu + 0.2 Al apfu, in accord with the formula unit calculated from the EMP analysis (Table 2).

Z site

The Z site potentially can be occupied by Mg, Al, and Fe^{3+}. In terms of X-ray diffraction, we can potentially represent the effective scattering species as Al* (= Al + Mg) and Fe, and the site populations of these aggregate species can be derived directly from the refined site-scattering values. For crystal 1, the amount of Al available to occupy the Z site (Table 2) is significantly less than the amount of Al* at Z as indicated from the refined site-scattering value, and hence there *must* be significant Mg at *Z*. Consequently, we must also allow for the difference in scattering between Mg (Z = 12) and Al (Z = 13) in crystal 1. Once this is done, we can express the Z site populations in terms of Al, Mg, and Fe* (= Fe^{2+} + Fe^{3+}), although these values for Al and Mg assume no Al-Mg disorder over the Y and Z sites.

Next, we need to use the <Z-O> distances to resolve the issue of possible Al/Mg disorder. Using the curve of <Z-O> vs. $\langle r^Z \rangle$ of Hawthorne et al. (1993), the Al/Mg site-populations of the Z sites were adjusted for linearity; the resulting site populations are given in Table 2.

Y site

The Y site potentially can be occupied by Li, Mg, Fe^{2+}, Mn^{2+}, Zn, Al, Fe^{3+}, and Ti^{4+}. In terms of X-ray diffraction, we can represent the effective scattering species as Al* (= Al + Mg) and Fe*(= Fe^{2+} + Fe^{3+}), with Li, Zn, and Ti contents taken from the unit-cell formula determined by microprobe analysis. The site populations of these aggregate species can be derived directly from the refined site-scattering values. The values for Mg, Al, Fe^{2+}, and Fe^{3+} are also determined from the unit-cell formula after subtracting the site populations assigned to the Z site. A comparison of the assigned site populations and the refined site-scattering values is given in Table 5. These results lie close to the relation between <Y-O> and $\langle r^Y \rangle$ proposed by Grice and Ercit (1993).

X site

The refined site-scattering values at the X site in all three crystals are in close agreement with the analogous values calculated from the microprobe data (Table 5). After convergence of the final refinement cycles for crystal 1, there was a maximum at 0, 0, 0.7673, with an electron density of 0.62 e–/ Å^3, 0.59 Å from X site, in the difference-Fourier map (Fig. 2). Attempts to refine an additional site were not successful.

The interpretation of this residual maximum is not straightforward. It could be interpreted as a splitting of the X site along the *c*-axis, related to occupancy of the W site by OH, F, or O^{2-}. Where an OH group is present at the W site, the O-H bond points toward the X site. Thus, depending on its size and charge, the cation at the X site could adopt different positions, depending on whether the W site was occupied by OH, F, or O^{2-}. Inspection of the data of Burns et al. (1994) shows that this feature is correlated with F content in elbaite. Possibly the split X site is associated with various locally ordered arrangements, in a similar fashion to the A site in amphiboles (Hawthorne et al. 1996).

ACKNOWLEDGMENTS

The authors thank C.A. Francis (Harvard Mineralogical Museum) and M.D. Dyar (West Chester University), who kindly provided the tourmaline samples, J. Stirling (Geol. Survey of Canada, Ottawa) for providing EMPA data for B, R. Gastoni for skillful sample preparation, and M. Palenzona for ion-probe maintenance. We also thank G.R. Rossman and M. Wise for their careful revision of the manuscript. The Consiglio Nazionale delle Ricerche is acknowledged for financing the ion microprobe at IGG (Pavia), whose facility was used in the present work. Financial support to F.C. from a FPU research fellowship of the Spanish M.E.C. is acknowledged. F.C.H. was supported by Major Installation and Research Grants from the Natural Sciences and Engineering Research Council of Canada.

REFERENCES CITED

Armstrong, J.T. (1988) Quantitative analysis of silicates and oxide minerals: Comparison of Monte Carlo, ZAF and Phi-Rho-Z procedures, Microbeam Analysis, Microbeam Analysis 1988, 239–246.

Blessing, R.H., Coppens, P., and Becker, P. (1974) Computer analysis of step scanned X-ray data. Journal of Applied Crystallography, 7, 488–492.

Bloodaxe, E.S., Hughes, J.M., Dyar, M.D., Grew, E.S., and Guidotti, C.V. (1999) Linking the structure and chemistry of the schorl-dravite series. American Mineralogist, 84, 922–928.

Burns, P.C., MacDonald, D.J., and Hawthorne, F.C. (1994) The crystal chemistry of manganese-bearing elbaites. Canadian Mineralogist, 32, 31–41.

Dyar, M.D., Taylor, M.E., Lutz, T.M., Francis, C.A., Guidotti, C.V., and Wise, M. (1998) Inclusive chemical characterization of tourmaline: Mössbauer study of Fe valence and site occupancy. American Mineralogist, 83, 848–864.

Foit, F.F. Jr. and Rossenberg, P.E. (1977) Coupled substitution in the tourmaline group. Contributions to Mineralogy and Petrology, 62, 109–127.

Frondel, C., Biedl, A., and Ito, J. (1966) New type of ferric iron tourmaline. American Mineralogist, 51, 1501–1505.

Grice, J.D. and Ercit, T.S. (1993) Ordering of Fe and Mg in the tourmaline crystal structure: the correct formula. Neues Jahrbuch für Mineralogie Abhandlungen, 165, 245–266.

Grice, J.D. and Robinson, G.W. (1989) Feruvite, a new member of the tourmaline group, and its crystal structure. Canadian Mineralogist, 27, 199–203.

Grice, J.D., Ercit, T.S., and Hawthorne, F.C. (1993) Povondravite, a redefinition of the tourmaline ferridravite. American Mineralogist, 78, 433–436.

Grew, E.S. (1996) Borosilicates (exclusive of tourmaline) and boron in rock forming minerals in metamorphic environments. In L.M. Anovitz and E.S. Grew, Eds., Boron: Mineralogy, Petrology and Geochemistry, 33, 387–501. Reviews in Mineralogy, Mineralogical Society of America, Washington, D.C.

Hawthorne, F.C. (1995) Light lithophile elements in metamorphic rock-forming minerals. European Journal of Mineralogy, 7, 607–622.

———(1996) Structural mechanisms for light-element variations in tourmaline. Canadian Mineralogist, 34, 123–132.

Hawthorne, F.C. and Henry, D.J. (1999) Classification of the minerals of the tourmaline group. European Journal of Mineralogy, 11, 201–215.

Hawthorne, F.C., MacDonald, D.J., and Burns, P.C. (1993) Reassignment of cation sites occupancies in tourmaline: Al/Mg disorder in the crystal structure of dravite. American Mineralogist, 78, 265–270.

Hawthorne, F.C., Oberti, R., and Sardone, N. (1996) Sodium at the *A* site in clinoamphiboles: the effects of composition on patterns of order, Canadian Mineralogist, 34, 577–593.

Henry, D.J. and Dutrow, B.L. (1996) Metamorphic tourmaline and its petrogenetic applications. In L.M. Anovitz and E.S. Grew, Eds., Boron: Mineralogy, Petrology and Geochemistry, 33, 503–557. Reviews in Mineralogy, Mineralogical Society of America, Washington, D.C.

Henry, D.J. and Guidotti, C.V. (1985) Tourmaline as a petrogenetic indicator mineral: an example from the staurolite grade metapelites of NW Maine. American Mineralogist, 70, 1–15.

Henry, D.J., Kirkland, B.L., and Kirkland, D.W. (1999) Sector-zoned tourmaline from cap rock of a salt dome. European Journal of Mineralogy, 11, 217–225.

Hervig, R.L. (1996) Analysis of geological materials for boron by secondary ion mass spectrometry. In L.M. Anovitz and E.S. Grew, Eds., Boron: Mineralogy, Petrology and Geochemistry, 33, 789–803. Reviews in Mineralogy, Mineralogical Society of America, Washington, D.C.

Lehmann, M.S. and Larsen, F.K. (1974) A method for location of the peaks in step-scan-measured Bragg reflections. Acta Crystallographica, A30, 580–584.

London, D., Morgan, D.B. VI, and Wolf, M.B. (1996) Boron in granitic rocks and their contact aureoles. In L.M. Anovitz and E.S. Grew, Eds., Boron: Mineralogy, Petrology and Geochemistry, 33, 299–329. Reviews in Mineralogy, Mineralogical Society of America, Washington, D.C.

McGee, J.J. and Anovitz, L.M. (1996) Electron probe microanalysis of geological materials for boron. In L.M. Anovitz and E.S. Grew, Eds., Boron: Mineralogy, Petrology and Geochemistry, 33, 771–788. Reviews in Mineralogy, Mineralogical Society of America, Washington, D.C.

McGee, J.J., Slack, J.F., and Herrington, C.R. (1991) Boron analysis by electron microprobe using MoB_4C layered synthetic crystals. American Mineralogist, 76, 681–684.

North, A.C.T., Phillips, D.C., and Mathews, F.S. (1968) A semi-empirical method of absorption correction. Acta Crystallographica, A24, 351–359.

Ottolini, L. and Hawthorne, F.C. (1999) An investigation of SIMS matrix effects on H, Li, and B ionization in tourmaline. European Journal of Mineralogy, 11, 679–690.

Ottolini, L., Cámara, F., Hawthorne, F.C., and Stirling, J. (2002) SIMS matrix effects in the analysis of light elements in silicate minerals: Comparison with SREF and EMPA. American Mineralogist, 87, 1477–1485.

Pouchou, J.L. and Pichoir, F. (1984) A new model for quantitative analyses. I. Application to the analysis of homogeneous samples, La Recherche Aérospatiale, 3, 13–38.

———(1985) "PAP" $\phi(\rho Z)$ procedure for improved quantitative microanalyses. Microbeam Analysis, 104–106.

Povondra, P. and Novák, M. (1986) Tourmalines in metamorphosed carbonate rocks from western Moravia, Czechoslovakia. Neues Jahrbuch für Mineralogie Monatshefte, 273–282.

Sheldrick, G.M. (1997) SHELXL-97: Program for Crystal Structure Refinement. Journal of Macromolecular Biology, 276.

Ungaretti, L., Lombardo, B., Domeneghetti, C., and Rossi, G. (1983) Crystal-chemical evolution of amphiboles from eclogitised rocks of the Sesia-Lanzo Zone, Italian Western Alps. Bulletin de Mineralogie, 106, 645–672.

Wilson, A.J.C., Ed. (1995) International Tables for Crystallography, Volume C, Kluwer Academic Publishers, Dordrecht, The Netherlands.

MANUSCRIPT RECEIVED NOVEMBER 10, 2000
MANUSCRIPT ACCEPTED APRIL 30, 2002
MANUSCRIPT HANDLED BY JEFFREY E. POST